



Effects of Truncating the Height of Compound Parabolic Collector on its Geometry, Optical and Thermal Performances

Bala ABDULLAHI^{1*}, Bala G. ABDURRAHMAN², Yusuf ALHASAN³, Saidu B. ABUBAKAR⁴, Bashir I. KUNYA⁵, Raya K. ALDADAH⁶, Saad MAHMOUD⁷, Ahmed REZK⁸

^{1*,3,4,5}Department of Mechanical Engineering, Kano University of Science and Technology, Wudil, Nigeria

²Department of Mechanical Engineering, Federal University of Technology, Minna, Nigeria

^{6,7}School of Mechanical Engineering, University of Birmingham, Birmingham, United Kingdom

⁸Energy and Bioproducts Research Institute (EBRI), College of Engineering and Physical Science, Aston University, Birmingham, UK, B4 7ET

*ibniabdallah12@gmail.com

Abstract

Radiation available, collector design and its orientation are the key parameters that affect the performance of any solar collector. At low concentrations, the concentrator of Compound Parabolic Collector (CPC) tends to be long and most of the top parts are not contributing to the radiation collection. Reducing the height (truncation) of those parts increases the optical efficiency at the expense of the concentration ratio. This work presents computational and experimental studies on the effects of truncation level of heat pipe-based compound parabolic collector (HPCPC) on its optical performance using solar radiation data from Kano, Nigeria (12.05°N). It aims to determine the effects of truncation at different truncation levels to determine the best level. Two computer programs were developed for the geometric characterization of symmetric low concentration compound parabolic collectors and for studying the effects of truncating its concentrator. Results showed that as the truncation levels increase, the collector height, aperture width, concentration ratio, and the average number of reflections decrease while the acceptance angle increases. The truncation effect was also studied using a validated advanced ray-tracing technique. Results showed that truncation increases the optical efficiency of the HPCPC but decreases its concentration ratio. From the graph of optic, low efficiency and concentration ratio against truncation level, results showed that the HPCPC with an acceptance angle of 60° and receiver radius of 12.5 (i.e. HPCPC60R12.5), HPCPC40R12.5 and HPCPC30R12.5 can be truncated respectively by 62%, 55% and 43% to achieve optical efficiencies/concentration ratios of 84%/1.65, 71%/2.55 and 55%/3.5.

Keywords: Truncation level, Optical Simulation, Optical efficiency, Concentration ratio, Acceptance angle.

1. Introduction

The use of renewable energy systems to harness solar radiation for different applications is getting more attention due to the pollution problems and the increasing costs of fossil fuels. In many countries, solar energy tends to be the most commonly used among all the renewable energy types. It is the most rapidly growing renewable source due to its advantages of flexibility, wide applications, low maintenance cost and versatility (Sambo and Bala, 2012). However, solar systems like other renewable systems are faced with the challenges of low efficiency; high initial cost and limited awareness (in some locations) (Sambo and Bala, 2012). Different solar energy systems particularly thermal and photovoltaic are used to harness the available solar radiation in many locations in the world. In some systems, concentrating systems such as compound parabolic collectors are used to capture more radiation in a relatively small area to reduce the total cost of the system (Rabl, 1985).

Compound Parabolic Collectors (CPC) are non-imaging collectors with high concentration ratios for a given acceptance angle. CPCs have properties of both concentrating and flat plate collectors with low alignment errors for reflective and receiving surfaces and high optical efficiency. After Winston's first design of CPC in 1974 (Abdullahi, 2015), research works were conducted using different design approaches to investigate its capabilities and advantages for different applications. Farouk et al. 1996 (Farouk et al., 1996) presented an asymmetric CPC with an inverted absorber. Ray tracing technique was used in analyzing the optical performance and the effects of the gap height on the optical efficiency and the convection heat losses and concluded that the optical efficiency decreases with an increase in the gap height. Comparative work between static evacuated CPCs and the tracking parabolic troughs was presented by Grass et al. 2004 (Grass et al., 2004). Their optical and thermal analysis showed that the tracking evacuated tube collector with an acceptance angle of 5.7° gave an optical efficiency of 71% against the 69% of the parabolic trough from Industrial Solar Technology (IST). However, a comparison between the tracking system's additional cost and the efficiency gain ought to be made in their work.

Since its invention, it was realised that CPCs usually have large reflector surface areas, and the top parts do not capture much radiation (Rabl, 1985) and hence can be cut. CPCs with truncated top parts were shown to

perform better than the untruncated counterpart, as reported by many researchers, but with little loss in concentration (Rabl, 1985). An internal low concentrating evacuated tube heat pipe solar collector with an acceptance angle of 20° was designed for powering solar air-conditioning systems (Nkwetta *et al.*, 2012) and their results showed that truncating the internal reflector reduced the cost of the system and the reflector losses. Almonacid *et al.* 1987 used the ray-tracing technique and studied the effects of truncation on static and adjustable CPC with bifacial cells filled with dielectric was presented by (Almonacid *et al.*, 1987). The irradiance gain, directional intercept and irradiance intercept factors were determined, and found that the truncated collector outperformed the full profile. Other works reported the influence of truncation on; energy collection (Carvalho, 1985), geometric characteristics (Rabl, 1976 and Kaligorous, 2009), and the intercept factor of the CPC-PV system (Almonacid, 1984). However, most works in the literature did not study the effects in detail, and instead, they based their truncation levels on the recommendations from past works, which suggested that the reflectors of CPCs can be cut by 50% with small effect.

Most of the studies reported in the literature lacked detailed studies on the truncation effects at various levels, which creates a gap in this vital aspect of performance improvement and cost reduction. Therefore, the current work aims to undertake detailed computational and experimental studies on the truncation effects on the CPC geometry, optical efficiency and the concentration ratio. To achieve the aim, the advanced ray tracing technique was extensively used for details studies on the effects of truncating a CPC collector on its optical performance, which led to determining the best truncation level for maximum optical efficiency and acceptable concentration. Furthermore, the simulation approach was validated by experimentation on a CPC constructed and tested indoors using an in-house solar simulator at the University of Birmingham, UK.

1. Geometry of the Heat Pipe Based Compound Parabolic Collector (HPCPC)

The geometries of the HPCPC with a cylindrical receiver can be generated using two inputs; the half acceptance angle (θ_a) and the receiver radius (r) (Chaves, 2008):

For the involute section:

$$\begin{aligned} x &= r(\pm \phi \cos \phi \pm \sin \phi) \\ y &= r(-\cos \phi - \phi \sin \phi) \end{aligned} \quad (1)$$

where

$$-\left(\frac{\pi}{2} + \theta_a\right) \subseteq \phi \subseteq 0$$

And for macro- focal parabola section;

$$\begin{aligned} x &= \frac{r}{\cos \phi - 1} \left[\pm \cos \theta_a \pm \cos(\phi - \theta_a) \pm \right. \\ &\quad \left. (2\pi - \phi + 2\theta_a) \sin(\phi - \theta_a) \right] \\ y &= \frac{r}{\cos \phi - 1} \left[(-2\pi + \phi - 2\theta_a) \cos(\phi - \theta_a) \right. \\ &\quad \left. - \sin(\phi - \theta_a) - \sin \theta_a \right] \end{aligned} \quad (2)$$

where $2\theta_a \subseteq \phi \subseteq \pi$

The half acceptance angle is related to the geometric concentration ratio C , as studied by Duffie and Beckham, 2006:

$$C = \frac{A_a}{A_r} = \frac{1}{\sin \theta_a} \quad (3)$$

Where A_a and A_r are the aperture and the receiver areas, respectively. The average number of reflections for full and truncated CPC is calculated as (Duffie and Beckham, 2006):

$$n_i = \max \left[C \frac{A_{RT}}{4a_T} - \frac{x^2 - \cos^2 \theta}{2(1 + \sin \theta)}, 1 - \frac{1}{C} \right] \quad (4)$$

$$x = \left(\frac{1 + \sin \theta}{\cos \theta} \right) \left(-\sin \theta + \left(1 + \frac{h_t}{h} \cot^2 \theta \right)^{1/2} \right) \quad (5)$$

where A_{RT} is the reflector area per unit depth of the truncated CPC, and C is the concentration ratio. Figure 1 shows a 2-D view of a HPCPC consisting of the major parameters that describe its concentrator, such as the acceptance angle, collector height and width. Equations 1 to 5 were employed to develop a computer program in excel spreadsheet® to determine the characteristics of the HPCPC geometry and study the effects of the truncation on the geometry of HPCPC. The same equations were coded in solidworks® software, and different geometries of HPCPC were generated. The characteristics of the HPCPCs from the two programs developed were found to be the same, and this validates the one developed in excel spreadsheet®. Table 1 shows the geometric characteristics of the HPCPC profiles generated using the model with acceptance angles of 20°, 30°, 40°, 50° and 60° and receiver radii of 11, 12.5, 22.5 and 25mm.

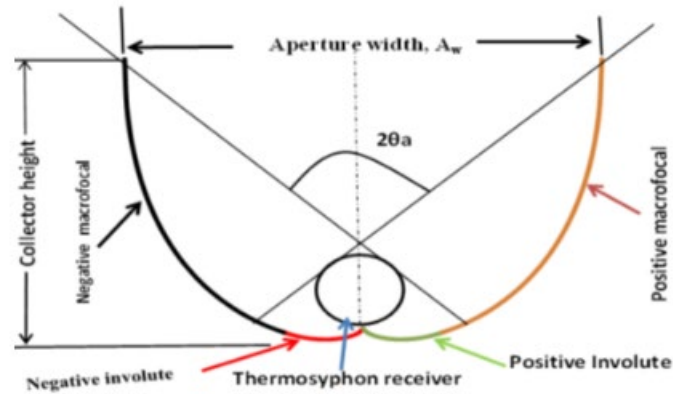


Figure 1 A 2-D view of the HPCPC

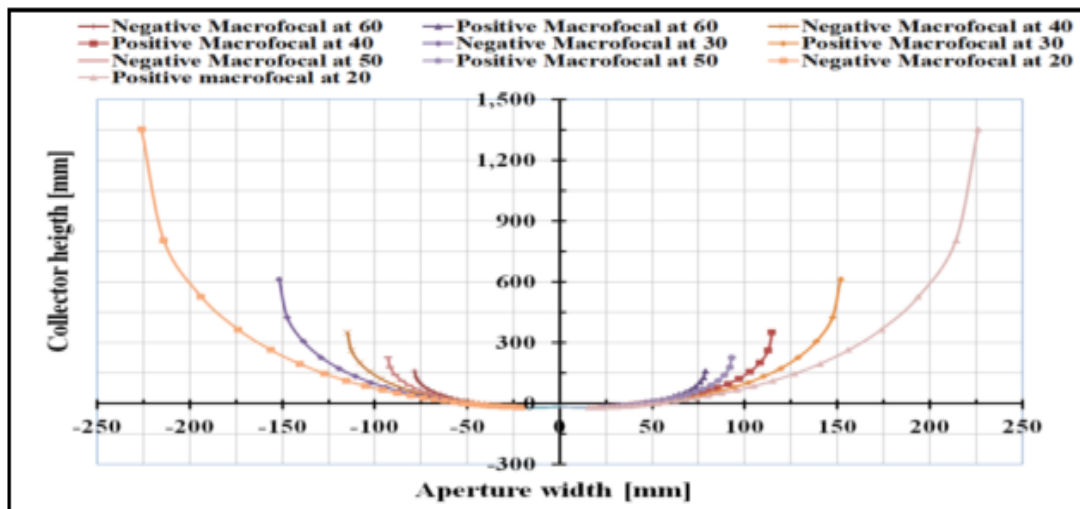


Figure 2 HPCPC generated with different acceptance angles and 12.5mm receiver radius

Figure 2 shows the generated HPCPC geometries from the model, with five different acceptance angles and a receiver radius of 12.5mm. It can be seen from Table 1 and Figure 2 that both the collector height and the aperture width increase as the receiver radius increases. Also, as the acceptance angle decreases, both the collector height, aperture width and the concentration ratio increase; thus, the larger the acceptance angle, the smaller the size of the concentrator.

Table 1 Geometric Characteristics of the CPC generated at different Acceptance angle and receiver radii

S/N	Receiver radius, r(mm)	Geometric Parameters	Acceptance angle, θ				
			60°	50°	40°	30°	20°
1	11	Collector height (mm)	159	218.7	327.02	558.07	1209.25
		Aperture width (mm)	138.23	163.54	202.08	267.04	398.02
		Concentration ratio	2	2.37	2.92	3.86	5.76
		Height to aperture ratio	1.15	1.34	1.62	2.09	3.04
2	12.5	Collector height (mm)	180.66	248.46	371.617	634.171	1374.15
		Aperture width (mm)	157.08	185.84	229.64	303.45	452.29
		Concentration ratio	2	2.37	2.92	3.86	5.76
		Height to aperture ratio	1.15	1.34	1.62	2.09	3.04
3	22.5	Collector height (mm)	325.796	447.24	668.91	1141.51	2473.48
		Aperture width (mm)	282.74	334.51	413.34	546.22	814.13
		Concentration ratio	2	2.37	2.92	3.86	5.76
		Height to aperture ratio	1.15	1.34	1.62	2.09	3.04
4	25.0	Collector height (mm)	361.329	496.94	743.234	1268.34	2748.31
		Aperture width (mm)	314.16	371.68	459.27	606.91	904.59
		Concentration ratio	2	2.37	2.92	3.86	5.76
		Height to aperture ratio	1.15	1.34	1.62	2.09	3.04

2.1 Effects of truncation on the geometry of HPCPC

The reflectors in CPC tend to be very large (as seen in the previous results), and the upper parts are parallel to the central plane of symmetry of the concentrator hence contributing little to the radiation reaching the absorber so that such part can be truncated without any significant effect on the performance of the collector. Hence, the CPC is truncated to reduce its height, which saves materials, space, and cost with little sacrifice in performance.

The developed model was employed to study the effect of truncation on the geometry of HPCPC whereby the heights of the heat pipe-based compound parabolic collector with 60° acceptance angle (HPCPC60), heat pipe based compound parabolic collector with 40° acceptance angle (HPCPC40) and heat pipe based compound parabolic collector with 30° acceptance angle (HPCPC30) with receiver radii of 12.5 and 25mm were truncated by 10, 30, 50 and 70%. Tables 2, 3 and 4 show the geometric characteristics of HPCPC60R12.5, HPCPC40R12.5 and HPCPC30R12.5 at different percentages of truncation (referred to as *truncation level*). Figure 3 shows samples of the generated profiles from solidworks® at different truncation levels. It can be seen from these tables that as the truncation level increases, the collector height, aperture width, average number of reflections, and height-to-aperture ratio decrease while the acceptance angle increases.

Table 2 Geometric characteristics of HPCPC60R12.5 at different truncation levels

Percentage truncated (%)	Collector Height (mm)	Aperture Width (mm)	Height-to-Aperture ratio	Concentration ratio	Half Acceptance Angle/°	Average number of reflection
0	180.65	157.08	1.15	2.00	30.00	0.500
10	162.58	156.60	1.04	1.99	30.17	0.497
30	126.45	152.30	0.83	1.94	31.00	0.485
50	90.33	141.99	0.64	1.81	33.50	0.448
70	54.20	122.14	0.44	1.56	39.87	0.359

Table 3 Geometric characteristics of HPCPC40R12.5 at different truncation levels

Percentage truncated (%)	Collector Height (mm)	Aperture Width (mm)	Height-to-Aperture ratio	Concentration ratio	Half Acceptance Angle/°	Average number of reflection
0	371.6	229.60	1.62	2.92	20.00	0.66
10	334.44	228.96	1.46	2.92	20.06	0.66
30	260.12	222.88	1.17	2.84	20.63	0.65
50	185.8	208.14	0.89	2.65	22.17	0.62
70	111.48	179.17	0.62	2.28	26.00	0.56

Table 4 Geometric characteristics of HPCPC30R12.5 at different truncation levels

Percentage truncated (%)	Collector Height (mm)	Aperture Width (mm)	Height-to-Aperture ratio	Concentration ratio	Half Acceptance Angle/°	Average number of reflection
0	634.20	303.50	2.09	3.86	15.00	0.74
10	570.78	302.59	1.89	3.85	15.04	0.74
30	443.94	294.73	1.51	3.75	15.45	0.73
50	317.10	275.55	1.15	3.51	16.56	0.71
70	190.26	237.57	0.80	3.02	19.30	0.67

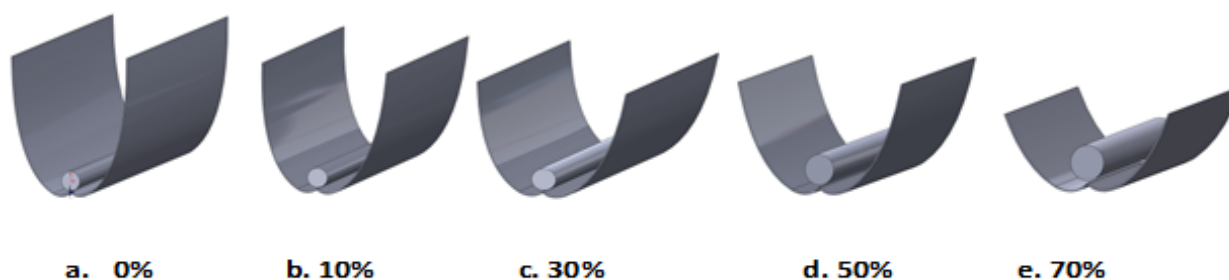


Figure 3 The Geometries of HPCPC60R12.5 at different truncation levels

Also, the concentration ratio of the HPCPC decreases by increasing the truncation level due to the increase in the acceptance angle. While the average number of reflections decreases with the increase in the truncation level due to the decrease in the concentration ratio, these trends are found to be the same for HPCPC40 and HPCPC30 (Tables 3 and 4). These results show that truncated HPCPC has a wider acceptance angle, lower concentration, and a low average number of reflections. Hence it can accept more radiation than the full profile and have fewer losses due to reflection.

3.0 Validation of the Optical Simulation Employed

3.1 Experiment

To validate the optical simulation approach used in section 4, an experimental test rig was built, which consists of a heat pipe-based compound parabolic collector with 60° acceptance angle and receiver radius of 11mm (HPCPC60R11), 400mm long thermosyphon heat pipe, radiant flux sensors, angular adjustment frame, DT85 data taker and other instrumentations. The geometry of HPCPC60R11 truncated by 60% was manufactured using the electric discharge machining (EDM) process in the school of Mechanical Engineering, University of Birmingham, UK and its characteristics are shown in Table 5. The truncated HPCPC60R11 was tested using an in-house continuous solar simulator built for testing solar systems. Figures 4 and 5 depict the experimental setup and its schematic diagram. The incoming and received irradiance were measured using a 5 x 5 mm high sensitive radiant flux sensors [sensitivity ranging from 0.0834 to 0.114 $\mu\text{V} (\text{W}/\text{m}^2)$] from Captec Enterprise® that gives out voltage signals which is converted to voltage signals in W/m^2 by DT85 data taker. The test was run at different inclination angles which represent the solar hour angles, and the performance was evaluated based on the optical efficiency.

Table 5 Geometric characteristics of full and truncated HPCPC60R11

Parameter	Full profile	Truncated profile
Acceptance angle (°)	60	67.5
Collector height (mm)	158.99	64
Receiver radius (mm)	11	11
Aperture width (mm)	138.23	116.16
Collector length	200	200
Aperture area (mm ²)	27646	23232
Receiver area (mm ²)	13823.01	13823.01
Concentration ratio	2	1.8
Reflectivity of the concentrator	60%	60%

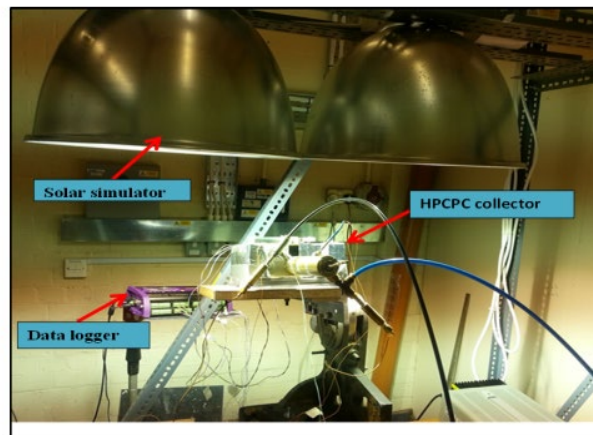


Figure 4 Photograph of the experimental setup for the Optical Performance test

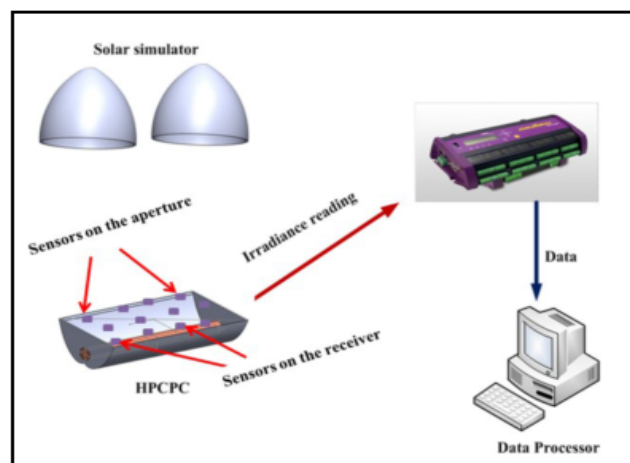


Figure 5 Schematic diagram of the test rig

3.2 Optical Simulation

The optical simulation was carried out using the procedure outlined in Figure 6 employing the properties stated in Table 5. The solar simulator was modelled as the Source, and the collector's performance was simulated at different solar hour angles between 45° and -45° . Figure 7 (a, b and c) shows incident rays, horizontal distribution of incoming and concentrated irradiance on the aperture and the receiver at 75° solar hour angle. The simulation results showed good agreement with experiment within $\pm 4.5\%$ deviation, as shown in Figure 8. This approach's validation was explained in detail in (Abdullahi *et al.*, 2015). However, the optical efficiency is low in this case due to the concentrator's low reflectivity (60%). This validated optical simulation approach is used in section 4 to study the truncation effects on the optical performance of different configurations of HPCPC.

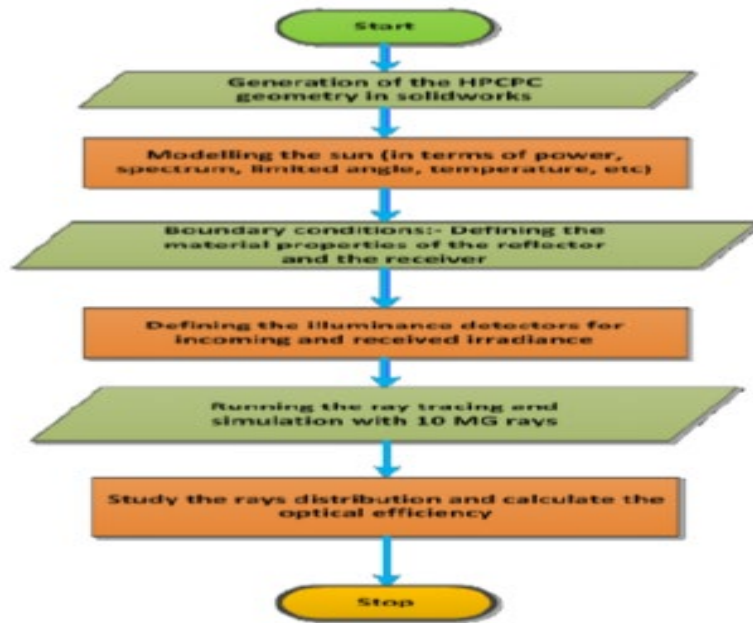
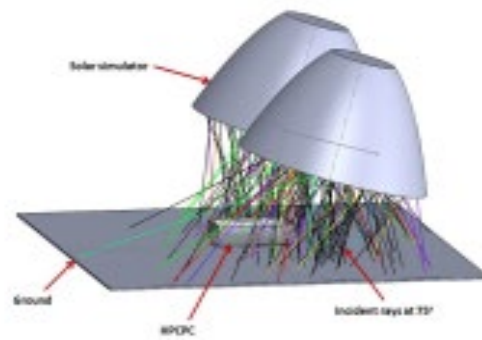
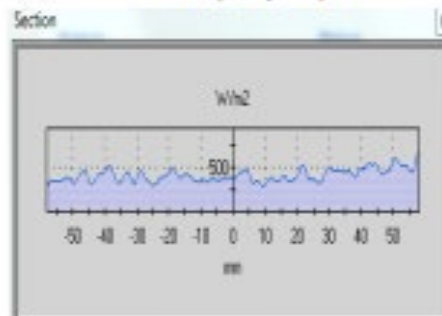


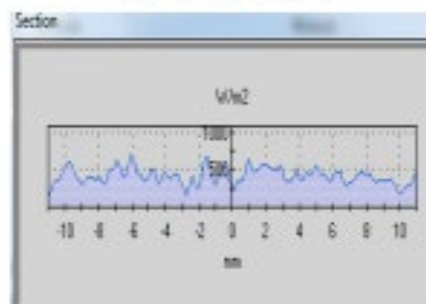
Figure 6 Flow chart of modelling process of HPCPC using ray tracing technique



a. Rays trajectory



b. Incoming irradiance



c. Top irradiance

Figure 7: Incident rays, incoming and received irradiance at 75° solar hour angle

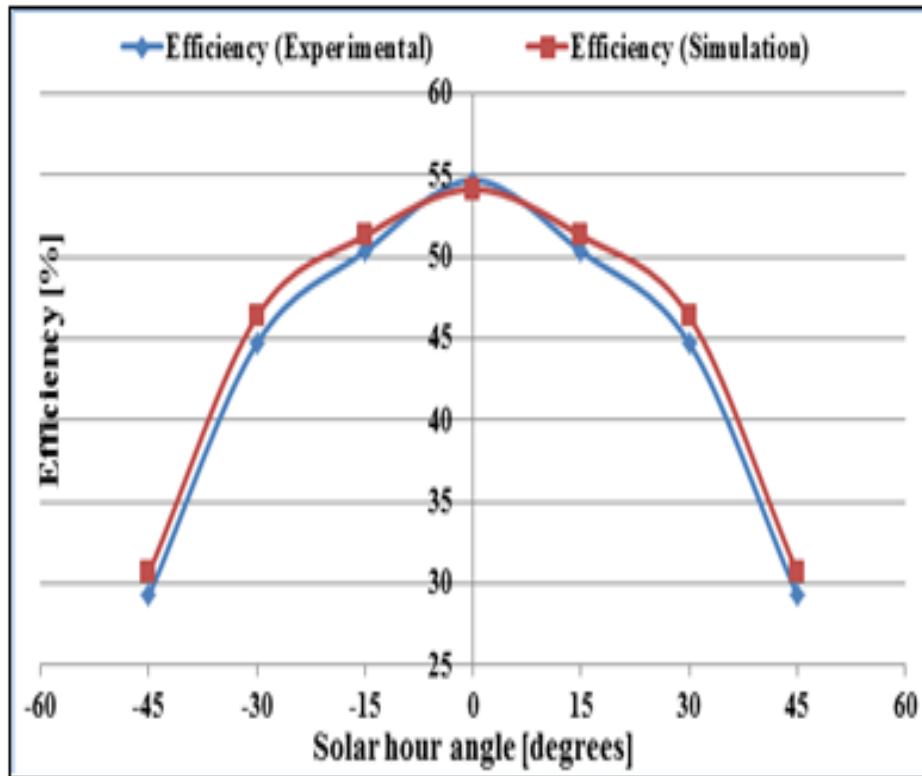


Figure 8: Optical efficiency of the HPCPC60R11 at different solar hour angles (simulation and experimental)

4.0 Optical Performance Evaluation of truncated HPCPC using ray tracing technique

The Ray tracing technique is a powerful tool that can be used to investigate the effect of truncation on the optical performance of HPCPC. This technique is used to determine the optical performance of solar systems, both thermal (Eames et al., 2001) and PV (Mallick, 2003) and (Sellami and Mallick, 2013) systems. The method is done with vectors by determining the direction and point of intersection of the incident ray with the reflecting surface and then the direction of the reflected rays, which follow the law of reflection as shown in Figure 9. Snell’s law described the behaviour of the refracting surfaces by defining the relationship between the angles of incidence and refraction for rays striking a surface between two media of different refractive indices.

The laws of reflection and refraction are applied to the ray tracing in solar systems and can be expressed in vector form as (Mallick, 2003):

$$\vec{r}_{ref} = \vec{i} - 2\left(\vec{i} \cdot \vec{n}\right)\vec{n} \tag{6}$$

$$n_r \vec{r}_{ref} = n_i \vec{i} + \left(n_r \vec{r}_{ref} \cdot \vec{n} - n_i \vec{i} \cdot \vec{n}\right)\vec{n} \tag{7}$$

The incident reflected and normal all laid on the same plane, and it is assumed that the incident and reflected rays make equal angles with normal (specular), as shown in Figure 9. Figure 9 shows one of the assumptions of ray tracing techniques (i.e. laws of reflection).

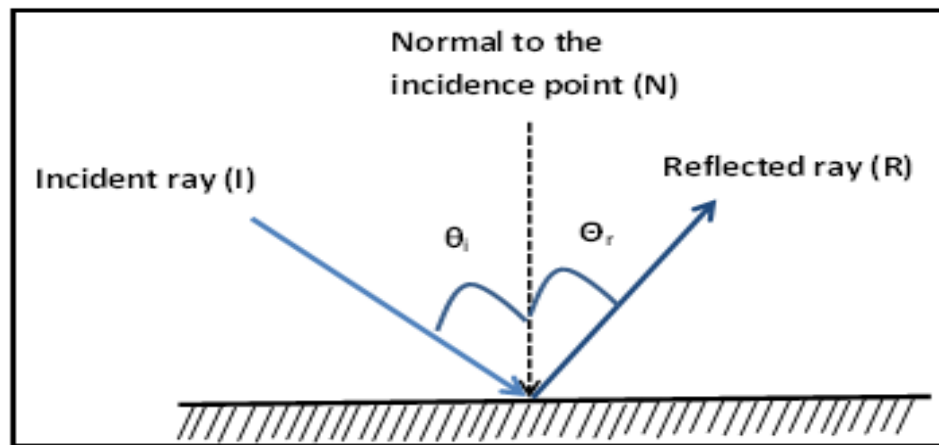


Figure 9: Laws of Reflection

Rays entering the CPC are either concentrated on the receiver or reflected back and exit the aperture as loss rays. This behaviour depends on the value of the ray's incident angle compared to the collector's half acceptance angle. All rays with an angle less than or equal to the half acceptance angle are reflected on the receiver, while those with angles greater than the half acceptance are reflected back and exit the aperture as a loss. The overall performance of the HPCPC in this work is evaluated in terms of its optical efficiency given by (Abdullahi *et al.*, 2014) :

$$\eta_o = \frac{\text{Power on the collector receiver}}{\text{Power on the collector aperture}} \quad (8)$$

The optical simulation carried out in this paper involves five major stages (as shown in Figure 7) which includes generating of the HPCPC profiles, modelling of the source (sun), defining material properties, defining the incoming and receiver detectors and running the ray tracing and simulation. Due to the nature of the receiver in this work (cylindrical), six detectors were used to identify the flux distribution on the top, bottom and the two sides of the receiver. The simulations were carried out according to the process outlined in Figure 7, and the source was set to generate 10 MW rays using the average radiation of November (699.59 W/m^2) at a tilt angle equal to the latitude of Kano (Abdullahi, 2015). The source was defined as planar, and its size was made larger than the aperture area of the collector so that the rays emitted cover the entire HPCPC aperture. The intensity type used was "Lambertian", and a limited half-angle of 0° was set for the source. Figure 10 shows the incidence rays from the model source, received and lost irradiance as it moves away from the zenith.

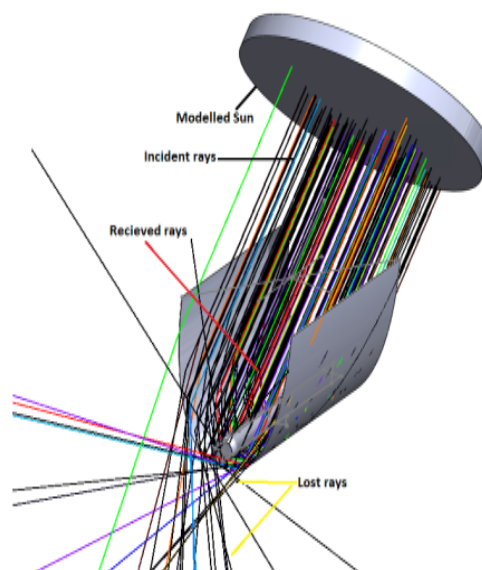


Figure 10: Incident rays from the modelled sun and the received and lost rays in the collector.

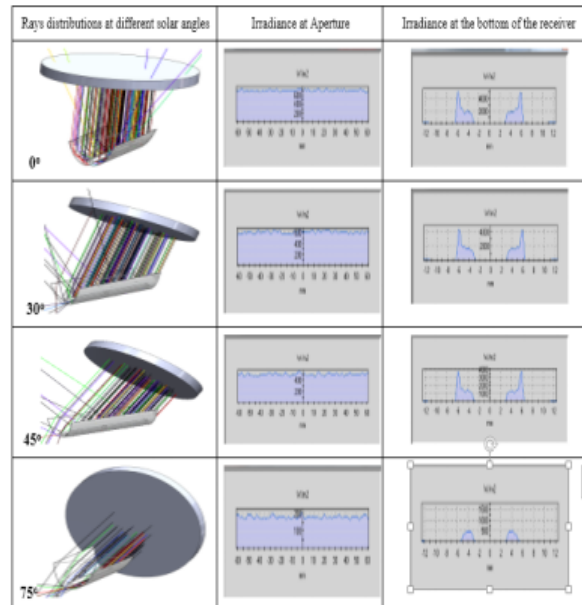


Figure 11| Rays distribution, the irradiance at the aperture and the bottom of the receiver at different sun hour angle

Figure 11 shows the distributions of rays within the CPC, irradiance on the aperture and irradiance on the bottom of the heat pipe receiver for sun hour angles of 0°(zenith), 30°, 45° and 75°. The figure shows that the amount of rays striking the collector reduces as the sun moves away from the zenith. Also, the intensity of the irradiance on the aperture decreases as the sun moves from 0° (700 W/m²) to 75° (228 W/m²).

Figure 11 also shows non-uniform irradiance distribution at the bottom of the thermosyphon heat pipe receiver with a high flux concentration at some points on the receiver surface, and this behaviour is more pronounced at sunrise and sunset. The concentration of the fluxes in such regions creates hot spots on the receiver, which can cause thermal losses due to the large temperature difference between the region and the ambient. The effects of the hot spot on the collector can be reduced by either locally changing the geometry of the receiver (creating a cavity) or altering the surface quality at the hot spots. Such results highlight the advantage of using the ray-tracing technique in the analysis and design of CPC collectors, where hot spot regions can be identified, and appropriate solutions can be applied.

Using this approach, the performance of six configurations of HPCPC with acceptance angles of 30°, 40° and 60° and two different receiver radii of 12.5 and 25mm each, truncated by 10, 30, 50 and 70% each, were simulated at different solar hour angles. Figures 12 (a, b and c) show the optical efficiency versus the sun hour angle at different truncation levels for the three out of the six configurations. There is an increase in optical efficiency in all the geometries as the truncation level increases (Figure 12). Hence the truncated geometries for all combinations of the acceptance angles and receiver radii perform better than the full geometry in terms of the optical efficiency. This improvement can be attributed to the decrease in the average number of reflections and increase in acceptance angle as the truncation level increases. When HPCPC is truncated, it can accept some rays out of the nominal acceptance angle, increasing optical efficiency. From such figures, the geometry of HPCPC60R12.5 truncated by 70% tends to be the best, with a collector height of 54.2 mm, aperture width of 122.14 mm and half acceptance angle of about 40° but with the lowest concentration ratio of 1.56. This geometry has the least average number of reflections of 0.4; hence the loss due to the multiple reflections of rays is minimized. Also, this geometry is the smallest and the most efficient (optically); hence it will occupy small space, use fewer materials and less cost, but with the least concentration ratio among the six simulated. The summary of the truncation effects on the HPCPC configurations with a receiver radius of 25 mm is shown in Table 6. It can be seen from such a table that similar effects were found with other configurations with a receiver of 12.5mm.

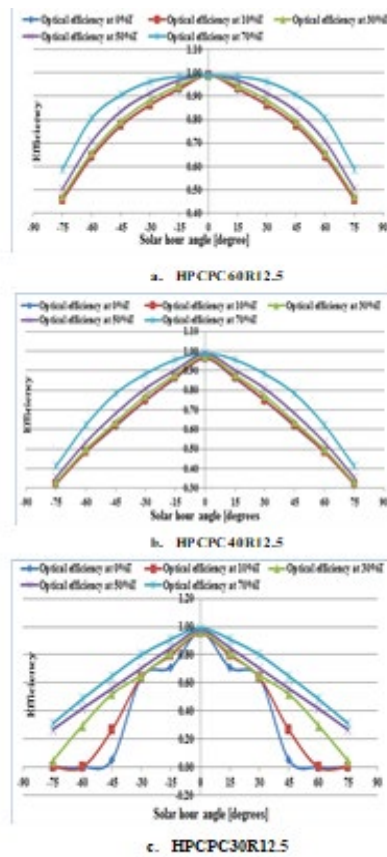


Figure 12 | Variation of optical efficiency with sun hour angle at different truncation levels

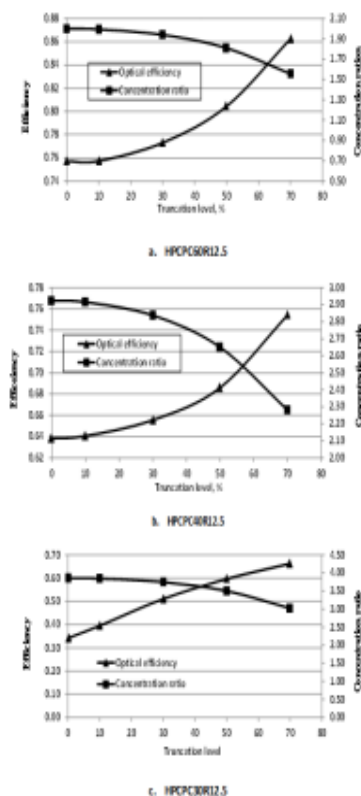


Figure 13 | Variation of average daily optical efficiency and concentration ratio with truncation level

Since the optical efficiency and concentration ratio show opposite effects as the truncation level increases, there is a need to have an optimum point where the best trend can be obtained. Figure 13 shows the daily average optical efficiency of different HPCPC configurations and concentration ratios at different truncation levels. The curves meet at different coordinates for the three configurations levels presented. For the wide acceptance angle of 60°, the

reflector can be truncated up to 62% with reasonable concentration (1.7) and optical efficiency (84%), while for acceptance angles of 40° (truncated by 57%) and 30° (43% truncated), the daily average optical efficiencies and concentration ratios will be 73%, 2.55 and 58%, 3.5 respectively. The charts in Figure 14 can be used as a guide for decision making between the percentage truncation to be used in comparison with the gain in the optical efficiency and the concentration ratio loss.

5.0 Thermal performance of the HPCPC

The experimental thermal performance of two configurations of the HPCPC with reflectivity of 60% (HPCPCR60) and 80% (HPCPCR80) and the concentration was carried out using a thermosyphon heat pipe as receivers.

5.1 Experimental test – up

Figures 14 and 15 show respectively a schematic diagram and pictorial view of the experimental test facility used for the thermal test. It consists of the two HPCPCs developed, 400mm long thermosyphon heat pipe, radiant flux sensor, angular adjustment frame, DT85 data taker and other instrumentations. It also has the cooling water circulating system used to extract the heat from the condenser section of the thermosyphon heat pipe. Surface thermocouples were installed on the tubes, and two probe thermocouples were installed at the inlet and outlet of the cooling water to measure the temperatures on the tube surface and the cooling water. The flow rate of the water is controlled by a valve and measured by a flow meter. The energy source is a continuous solar simulator designed for indoor testing of the HPCPC.

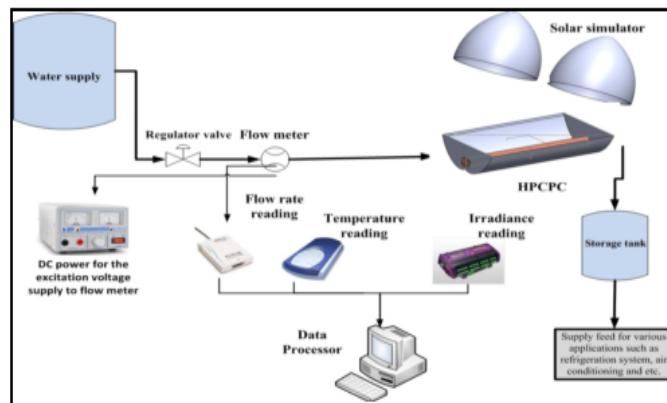


Figure 14 Schematic diagram of the test rig for the optical and thermal performance of HPCPC

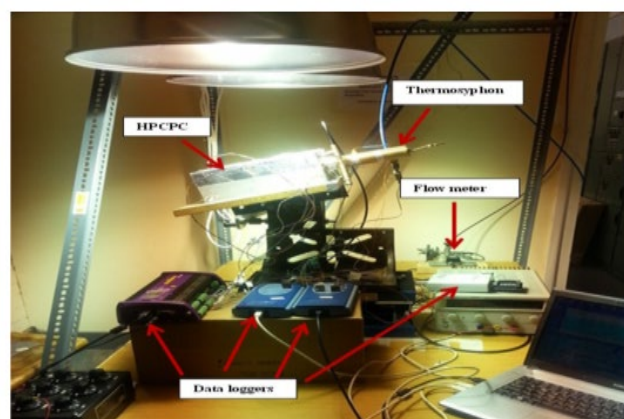


Figure 15 Photograph of the experiment on the effects of inclination angle of thermosyphon

5.2 Experimental procedure

The solar simulator is switched on and allowed to stabilize for one hour, and the incoming irradiance was measured using the radiant flux sensors by mapping the aperture area while the received irradiance was measured on four sides of the tube.

The performance of two HPCPCs; with reflectivity of 60% (HPCPCR60) and 80% (HPCPCR80), were investigated. Cooling water was circulated at an average flow rate of 0.0018 kg/s through the water jacket to

remove heat from the condenser section. Reading of the water flow rate, irradiance, ambient, surface, inlet and outlet temperature were recorded for each run. The experiments were repeated to prove the repeatability of the measurements. The test was run at irradiance, of 1067.71 W/m² and the rate of heat transfer to the cooling water at different inclinations of the thermosyphon was calculated for the two collectors using equation 21, and the result is presented in Figure 17.

$$Q_{out} = \dot{m} C_p (T_{out} - T_{in}) \quad (9)$$

where \dot{m} is the water mass flow rate, kg/s and C_p is the specific heat capacity of water, kJ/kg-K, while T_{in} and T_{out} are the average inlet and outlet cooling water temperatures, respectively.

It can be observed from the figure that up to 27% maximum improvement in heat transfer is achieved with HPCPCR80 compared to HPCPC60.

1

6. Conclusions

Different configurations of symmetric CPCs with different acceptance angles and receiver radius were characterized in terms of collector height, aperture width, concentration ratio, and the average number of reflections. For studying the effects of truncating the concentrator of the HPCPC using two computer models were developed in Microsoft excel[®] and coded solidworks[®] software.

The ray-tracing technique is a powerful tool for the optical evaluation of HPCPC collectors in predicting their optical efficiency at various sun hour angles and identifying areas of high irradiance intensities like hot spots. The optical simulation was carried out using this technique to study the effects of truncation on the optical performance of different configurations of the HPCPC. Results showed that truncating the height of the HPCPC reduces the height to aperture ratio, the average number of reflections and the geometric concentration ratio but increases its acceptance angle. The truncated HPCPC was found to have higher optical efficiency than the full one but with a lower geometric concentration ratio due to the increase in the acceptance angle. Generally, the results obtained showed that the acceptance angle of the HPCPC is very important in determining its optical and geometric characteristics.

Optically, the best geometry was found to be the one with the original height truncated by 70% for all the configurations, and such collector will be small, uses less material and gives the highest daily average optical efficiency (85%) but with the lowest concentration ratio (1.56) and can operate satisfactorily throughout the day without tracking the sun.

The optical efficiency and concentration ratio intersection points can be considered the best truncation that balances optical efficiency and the concentration ratio (as shown in Figure 14). It can be concluded from such figure that at the intersection points, the HPCPC60R12.5, HPCPC40R12.5 and HPCPC30R12.5 can be truncated respectively by 62%, 55% and 43% to achieve optical efficiencies/concentration ratios of 84%/1.65, 71%/2.55 and 55%/3.5 respectively. However, the choice of truncation level will depend on the priority between optical efficiency and concentration ratio for the proper operations of the system.

Results from the thermal performance experiment showed that a maximum improvement of up to 27% in heat transfer to the cooling water was achieved with HPCPCR80 compared to HPCPC

Acknowledgements

The first author acknowledged the financial support of Kano University of Science and Technology, Wudil, Kano – Nigeria and the Tertiary Education Trust fund (TETFUND), Abuja – Nigeria.

References

- Abdullahi, B., R.K. Al-dadah, and M. Saad, Optical Performance of Double Receiver Compound Parabolic Concentrator. *Energy Procedia*, 2014. 61(0): p. 2625-2628.
- Abdullahi, B., R.K. Al-dadah, and M. Saad, Optical and Thermal performance of double receiver compound parabolic concentrator. *Applied Energy*, 2015. 159: p. 1-10.
- Abdullahi, B., Development and Optimization of Heat pipe based of Compound Parabolic Collector, PhD Thesis submitted to the School of Mechanical Engineering 2015, University of Birmingham, UK, p. 287.
- Almonacid, G., Truncation effect of bifacial Compound Parabolic Concentrators. *Solar cells*, 1987. 22: p. 47 – 54.
- Almonacid, G., A. Luque, and A.G. Molledo, Photovoltaic static concentrator analysis. *Solar Cells*, 1984. 13(2): p. 163 - 178.
- Carvalho, M.J., et al., Truncation of CPC solar collectors and its effect on energy collection. *Solar Energy*, 1985. 35(5): p. 393-399.
- Chaves, J., *Introduction to Nonimaging Optics*. 2008, USA: CRC Press Taylor and Francis Group

- Duffie, J.A. and W.A. Beckham, *Solar Engineering of thermal processes*. 3rd ed. 2006, USA: John Wiley & son Inc.
- Eames, P.C., M. Smyth, and B. Norton, The experimental validation of a comprehensive unified model for optics and heat transfer in line-axis solar energy systems. *Solar Energy*, 2001. 71(2): p. 121-133.
- Farouk, K.A., P.C. Eames, and B. Norton, Optical performance of an asymmetric inverted absorber compound parabolic concentrating solar collector. *Renewable Energy*, 1996. 9: p. 576 - 579.
- Grass, C., et al., Comparison of the optics of non-tracking and novel types of tracking solar thermal collectors for process heat applications up to 300 °C. *Solar Energy*, 2004. 76(1-3): p. 207-215.
- Kaligorous, S., *Solar Energy Engineering: Processes and systems*. 2009, Academic press: Elsevier Science.
- Mallick, T.K., *Optics and Heat Transfer for Asymmetric Compound Parabolic Photovoltaic Concentrators for Building Integrated Photovoltaics in Faculty of Engineering*2003, University of Ulster.
- Nkwetta, D., et al., Optical evaluation and analysis of an internal low-concentrated evacuated tube heat pipe solar collector for powering solar air-conditioning systems. *Renewable Energy*, 2012. 39(1): p. 65-70.
- Rabl, A., Optical and thermal properties of compound parabolic concentrators. *Solar Energy*, 1976. 18(6): p. 497-511.
- Rabl, A., *Active Solar Collectors and their Applications*. First ed. 1985, New York: Oxford University Press
- Sambo, A.S. and E.J. Bala. Penetration of Solar Photovoltaic into Nigeria's Energy supply mix. in *World Renewable Energy Forum (WREF)*. 2012. Denver, Colorado USA: Curran Association Inc.
- Sellami, N. and T.K. Mallick, Optical efficiency study of PV Crossed Compound Parabolic Concentrator. *Applied Energy*, 2013. 102(0): p. 868-876.
- Winston, R., Principles of solar concentrators of a novel design. *Solar Energy*, 1974. 16(2): p. 89-95.